DALTON

Crystal structure and magnetic properties of the layer ferrimagnet $N(n\text{-}C_5H_{11})_4Mn^{II}Fe^{III}(C_2O_4)_3$†

Simon G. Carling,[a] Corine Mathonière,[a] Peter Day,*[,a] K. M. Abdul Malik,[b] Simon J. Coles[b] and Michael B. Hursthouse[b]

[a] *Davy Faraday Research Laboratory, The Royal Insitution of Great Britain, 21 Albemarle Street, London W1X 4BS, UK*
[b] *School of Chemistry and Applied Chemistry, University College of Wales, Cardiff CF1 3TB, UK*

The crystal structure and magnetic properties of the molecular-based ferrimagnet $N(n\text{-}C_5H_{11})_4Mn^{II}Fe^{III}(C_2O_4)_3$ have been determined. The compound is orthorhombic, space group $C222_1$, $a = 9.707(3)$, $b = 16.140(3)$, $c = 19.883(7)$ Å (120 K), $Z = 4$ [R 0.047 for $I > 2\sigma(I)$]. The structure consists of hexagonal layers of alternating Mn^{II} and Fe^{III} bridged by $C_2O_4{}^{2-}$, separated by layers containing only $N(n\text{-}C_5H_{11})_4{}^+$ with the alkyl chains extended, though with the terminal bonds twisted towards the *gauche* conformation. The terminal CH_3 are embedded in the hexagonal pockets formed by three $C_2O_4{}^{2-}$. Since both metal ions have $3d^5$ configuration with ${}^6A_1$ ground states the magnetic properties in the paramagnetic region mimic those of a two-dimensional antiferromagnet. Below $T_N = 27$ K an uncompensated moment estimated as 8.78×10^{-5} μ_B atom^{-1} arises, the direction of which was identified as parallel to the c axis by single-crystal magnetization measurements.

In the search for new molecular-based magnets the oxalate ion is an attractive building block because its ambidentate co-ordinating ability enables it to form an exchange pathway between two metal ions. Discrete dimeric complexes have been synthesized to study the detail of the exchange process[1,2] but recently compounds have been reported in which oxalate ions are used to create bimetallic arrays that are infinite in two or three dimensions.[3,4] Magnetic exchange between moments localized on the two different metal ions may be ferro- or antiferro-magnetic according to their respective electron configurations, in conformity with the Kanamori–Goodenough rules.[5] The lattice topologies may also be highly unusual, for example the hexagonal honeycomb type in the case of the two-dimensional arrays or helical in the three-dimensional ones.[6,7] Such materials may also be interesting by reason of their optical transparency, since this carries the possibility of unusual optical phenomena resulting from the onset of magnetic order.[8] Finally, the synthetic opportunity to combine organic molecular species with inorganic complexes in the same lattice brings with it the chance of effecting very subtle influences on the ligand-field symmetry through small changes in molecular packing.

A further consequence of using molecular ligands to create ordered magnetic arrays is that a lowering of the ligand-field symmetry may induce single-ion anisotropy, which competes with exchange to give non-collinear magnetic structures.[9] The latter phenomenon, called spin canting or weak ferromagnetism, means that even antiferromagnetic near-neighbour exchange can result in an ordered array of moments with finite zero-field (spontaneous) magnetization. We have shown that even ions with orbital-singlet ground states can give rise to weakly ferromagnetic compounds: in the series $Mn(C_nH_{2n+1}PO_3)\cdot H_2O$ the size of the uncompensated moment, as well as the ordering temperature T_N, can be made to vary by changing the number of C atoms in the alkyl sidechain.[10] More recently we demonstrated[11] that in an extensive series of bimetallic oxalates $AMn^{II}Fe^{III}(C_2O_4)_3$, where A^+ is an organic cation, the degree of spin canting also changes markedly with A.

The latter compounds have the two-dimensional hexagonal arrangement of 3d ions referred to above, with the A^+ interleaving the layers, but while the broad outlines of the structures are clear from X-ray powder-diffraction data the fine detail is not. In the present paper we therefore report a single-crystal structure of one member of this series [$A = N(n\text{-}C_5H_{11})_4$]. The compound is a ferrimagnet, but because of the unusual circumstance that Mn^{II} and Fe^{III} are both $3d^5$ ions with the same ${}^6A_1$ ground state, the magnetic order mimics that of a two-dimensional antiferromagnet very closely. We also report single-crystal magnetization data at low temperature showing the magnitude and direction of the uncompensated moment.

Experimental

Preparation

Chemicals were standard reagents from Aldrich (≥99% purity). The compound $K_3Fe(C_2O_4)_3\cdot 3H_2O$ was prepared by the literature method.[12] Crystals of $N(n\text{-}C_5H_{11})_4MnFe(C_2O_4)_3$ were grown by weighing 1–2 mmol each of $K_3Fe(C_2O_4)_3\cdot 3H_2O$ and $MnSO_4\cdot 7H_2O$ into one arm of an H-shaped tube and $N(n\text{-}C_5H_{11})_4Br$ (1 mmol) in the other. Both vertical arms of the tube were then carefully filled with water so that the connecting horizontal tube was also filled, but no immediate mixing of the two components occurred. The tube was then left to stand in the dark at room temperature so that the reactants slowly diffused together over a period of 2 months yielding a small number of plate-like crystals. A polycrystalline sample of the product was checked by X-ray powder diffraction (Siemens D500) for the absence of impurities of iron or manganese oxides.

Crystallography

X-Ray diffraction data were collected at 120 K from a single crystal 0.28 × 0.24 × 0.11 mm by a four-circle diffractometer at the University College of Wales, Cardiff equipped with a Delft Instruments FAST TV area detector using graphite-monochromated Mo-Kα radiation (λ 0.710 69 Å) from a rotating-anode generator. Values of the lattice parameters were initially determined from the Bragg angles of 50 reflections. 6447 Reflections were measured, of which 2432 were independent.

The structure was refined by direct methods using SHELXL

---

† *Non-SI units employed:* G = 10^{-4} T, $\mu_B \approx 9.27 \times 10^{-24}$ J T^{-1}.

Table 1 Crystal data and structure-refinement parameters of N(n-C$_5$H$_{11}$)$_4$MnFe(C$_2$O$_4$)$_3$

Empirical formula	C$_{26}$H$_{44}$FeMnNO$_{12}$
M	673.41
Crystal system	Orthorhombic
Space group	$C222_1$
a/Å	9.707(3)
b/Å	16.140(3)
c/Å	19.883(7)
U/Å^3	3115(2)
Z	4
D_c/Mg m^3	1.436
μ/mm^{-1}	0.930
F(000)	1416
θ Range for data collection/°	2.45–25.04
hkl Ranges	−6 to 11, −18 to 18, −21 to 21
Reflections collected	6447
Independent reflections	2432 [R(int) = 0.0549]
Data, restraints, parameters	2431, 20, 174
Goodness of fit on F^2	0.970
$R1$, $wR2$ [$I > 2\sigma(I)$]	0.0473, 0.1147
(all data)	0.0619, 0.1240
Absolute structure parameter	0.45(8)
Largest difference peak and hole/e Å^{-3}	0.860, −0.333

Table 2 Atomic coordinates (×10^4) for N(n-C$_5$H$_{11}$)$_4$MnFe(C$_2$O$_4$)$_3$

Atom	x	y	z
Fe(1)	0	1706(1)	2500
Mn(2)	5000	3292(1)	2500
O(1)	−610(6)	672(4)	3094(3)
O(2)	−660(5)	−716(3)	3092(3)
O(3)	−1155(7)	2535(3)	3090(3)
O(4)	−1796(6)	1829(4)	1918(3)
O(5)	−3212(6)	3179(4)	3095(3)
O(6)	−3832(7)	2470(3)	1928(3)
C(1)	−359(3)	−23(8)	2844(2)
C(2)	−2317(10)	2714(6)	2848(5)
C(3)	−2682(10)	2310(6)	2170(5)
N(1)	3953(4)	5000	0
C(11)	3094(12)	5276(6)	604(5)
C(12)	1955(12)	4692(8)	811(6)
C(13)	1166(4)	5048(6)	1399(2)
C(14)	207(15)	4360(9)	1192(7)
C(15)	−784(19)	4237(13)	1769(9)
C(11′)	3023(15)	4662(8)	559(7)
C(12′)	2156(12)	5342(6)	861(5)
C(13′)	1166(4)	5048(6)	1399(2)
C(14′)	21(12)	5601(8)	1145(5)
C(15′)	−947(13)	5849(8)	1702(6)
C(21)	4768(14)	5761(8)	242(6)
C(22)	5849(10)	6090(6)	−238(4)
C(23)	6848(12)	6677(7)	102(7)
C(24)	7843(13)	7161(7)	−328(7)
C(25)	8689(16)	6579(8)	−756(7)
C(21′)	4896(12)	5689(6)	−267(5)
C(22′)	5887(24)	6091(15)	219(8)
C(23′)	6668(19)	6706(11)	−212(9)
C(24′)	7631(19)	7174(13)	248(11)
C(25′)	8766(19)	6701(11)	597(10)

Table 3 Selected bond lengths (Å) and angles (°) for N(n-C$_5$H$_{11}$)$_4$MnFe(C$_2$O$_4$)$_3$

Fe(1)–O(3)	2.103(6)	Mn(2)–O(6)	2.083(6)
Fe(1)–O(1)	2.129(6)	Mn(2)–O(2)	2.087(6)
Fe(1)–O(4)	2.102(6)	Mn(2)–O(5)	2.108(6)
O(1)–C(1)	1.250(12)	O(2)–C(1)	1.257(12)
O(3)–C(2)	1.260(11)	O(4)–C(3)	1.262(10)
O(5)–C(2)	1.248(10)	O(6)–C(3)	1.243(12)
C(1)–C(1′)	1.534(8)	C(2)–C(3)	1.540(5)
O(3′)–Fe(1)–O(3)	101.0(3)	O(3)–Fe(1)–O(4′)	94.3(3)
O(3)–Fe(1)–O(4)	78.7(2)	O(4′)–Fe(1)–O(4)	169.2(4)
O(3′)–Fe(1)–O(1)	163.1(2)	O(3)–Fe(1)–O(1)	92.4(2)
O(4′)–Fe(1)–O(1)	90.0(2)	O(4)–Fe(1)–O(1)	98.5(2)
O(1)–Fe(1)–O(1′)	76.7(3)	O(6″)–Mn(2)–O(6′)	100.8(3)
O(6′)–Mn(2)–O(2)	164.4(2)	O(6)–Mn(2)–O(2)	90.8(2)
O(2)–Mn(2)–O(2′)	79.8(3)		
O(6)–Mn(2)–O(5′)	94.9(3)	O(2″)–Mn(2)–O(5′)	97.5(2)
O(6)–Mn(2)–O(5)	78.7(3)	O(2″)–Mn(2)–O(5)	90.2(2)
O(5)–Mn(2)–O(5′)	170.0(3)		
C(1)–O(1)–Fe(1)	115.4(5)	C(1)–O(2)–Mn(2)	113.0(5)
C(2)–O(3)–Fe(1)	114.3(6)	C(3)–O(4)–Fe(1)	113.9(6)
C(2′)–O(5)–Mn(2)	113.9(6)	C(3′)–O(6)–Mn(2)	114.2(6)

93[13] with a full-matrix least-squares method on F^2 with 174 parameters to a final R value of 0.0473 based on reflections with $I > 2\sigma(I)$. Data were corrected for Lorentz and polarization factors and also for absorption. The non-hydrogen atoms were refined with anisotropic thermal parameters while the hydrogen atoms were refined freely with individual U_{iso} values. The weighting scheme used was $w = 1/\sigma^2(F_o^2)$. Scattering factors were taken from ref. 13. Crystal data are given in Table 1, positional parameters in Table 2 and selected bond lengths and angles in Table 3.

Complete atomic coordinates, thermal parameters and bond lengths and angles have been deposited at the Cambridge Crystallographic Data Centre. See Instructions for Authors, *J. Chem. Soc., Dalton Trans.*, 1996, Issue 1.

Magnetic measurements

Magnetic susceptibility and magnetization were measured using a Quantum Design MPMS 7 SQUID susceptometer. Data in the paramagnetic regime were recorded at a field of 1000 G on a polycrystalline sample mounted in a gelatine capsule. Below 30 K measurements were also made at 100 G on a single crystal, mounted in a Perspex rod that had been split in the centre to provide a cavity. The moment of the single crystal was corrected for the diamagnetism of the rod, and the core diamagnetism of the sample using Pascal's constants. Values of the Curie and Weiss constants in the paramagnetic region were derived by least-squares fitting of 31 data points between 150 and 300 K, the diamagnetism of the gelatine capsule being allowed for by measuring the empty capsule.

Results and Discussion

Crystal structure

The crystal structure of N(n-C$_5$H$_{11}$)$_4$MnFe(C$_2$O$_4$)$_3$ consists of alternate layers of [MnFe(C$_2$O$_4$)$_3$]$^-$ and N(n-C$_5$H$_{11}$)$_4{}^+$. The former comprise honeycomb networks of alternating Mn and Fe bridged by C$_2$O$_4{}^{2-}$ (Fig. 1). Thus both metal ions are co-ordinated by six O originating from three bidentate oxalate ions forming a trigonally distorted octahedron. Similar networks have been observed in PPh$_4$MnCr(C$_2$O$_4$)$_3$[4] and NBu$^n_4$MnCr(C$_2$O$_4$)$_3$[7] though in the latter case none of the C atoms of the quaternary ammonium cation was located, and the N was arbitrarily placed on a three-fold axis. In contrast we have been able to position all the C atoms of the N(n-C$_5$H$_{11}$)$_4{}^+$ and have not assumed a rhombohedral cell. In the PPh$_4{}^+$ compound, too, one P–C bond lies parallel to a three-fold axis and the unit cell is also rhombohedral. Thus we are in a position to discuss the co-ordination geometry of the metal ions and the packing of the organic cations in this class of compound in more detail than previously.

As far as the bimetallic tris(oxalato) layer is concerned (Fig. 1), the deviation of the 3d ions from a hexagonal array is implicit in the orthorhombic space group: the ratio b/a is 1.689:1 instead of the ideal value of 1.732:1 for a regular hexagonal lattice. Shortening of the hexagons along the twofold axis parallel to b therefore translates into a difference between the angles Fe–Mn–Fe and Mn–Fe–Mn (respectively 112 and 138°) instead of 120°. The site symmetry of the metal ions, which would be D_3 if the cell were rhombohedral, is reduced to C_2. This lowering of symmetry is manifested by the fact that the metal–oxygen bond lengths are not all equal: at both iron and manganese sites two bonds are slightly longer than the other four. At the Fe the other four bonds are equal within the standard deviation [two at 2.103(6) and two at 2.102(6) Å] while the remaining two, which are *cis* to one another and link the same oxalate ion, are 2.129(6) Å. In contrast, at the Mn we find two at 2.083(6), two at 2.087(6) and two at 2.108(6) Å, the longer pair of bonds in this case being *trans* to one another, and hence linking different oxalate ligands. At the manganese site the mean metal–oxygen bond length is 2.092 Å while at the Fe it is 2.111 Å. One index of the extent of distortion of the MO_6 units from regular octahedra is the deviation of the *trans* O–M–O bond angles from 180°: at the iron site we find two such angles are 163 and one 169°, *i.e.* essentially equal distortions. As expected for bidentate chelating oxalate groups the 'bite angle' O–M–O is considerably less than 90°, averaging 78.0° around the Fe and 79° around the Mn. These figures compare quite closely with those found in other oxalato-complexes of Fe^{III} and Mn^{II}.[1] In view of these small angles it is still possible to discuss the distortion from octahedral co-ordination despite the fact that the site symmetry is C_2 rather than D_3. For example the question arises whether the octahedra are trigonally elongated or compressed along what would have been the three-fold axis. Since the mean O–M–O angle for O atoms on adjacent oxalate groups exceeds 90° (99.4° at the Fe and 98.6° at Mn) both MO_6 octahedra may be considered as slightly elongated perpendicular to the plane of the $[MnFe(C_2O_4)_3]^-$ layer.

It has been noted that in other bimetallic tris(oxalato) compounds with layer structures[4,7] it is a condition for the existence of a honeycomb network of ambidentate oxalate groups that the configurations about the two metal ion sites should be of opposite chirality. A similar circumstance obtains in the present case. However, the compounds in question were synthesized from racemic starting materials. In the structure of the $N(n\text{-}C_5H_{11})_4$ compound we find that alternate layers have opposite chirality [*i.e.* Mn(Λ) and Fe(Δ) in one layer, and Mn(Δ), Fe(Λ) in the next] (Fig. 2). We are currently synthesizing bimetallic tris(oxalato) compounds of different 3d ions from chiral starting materials so as to obtain fully chiral products.

Turning to the disposition of the organic cations, we find a most intricate and unusual arrangement. The N atoms of the $N(n\text{-}C_5H_{11})_4^+$ form rectangular planar arrays, interleaving the $MnFe(C_2O_4)_3^-$ layers, with the four attached alkyl chains extended two in the plane of the N and two perpendicular. The first four C atoms in each chain are in a fully extended *trans* configuration but the terminal CH_3 is twisted away from the plane described by the four CH_2 partly towards the *gauche* configuration (Fig. 3). It is interesting that our attempts to synthesize compounds in the series $N(n\text{-}C_nH_{2n+1})_4MnFe(C_2O_4)_3$ were only successful for $n = 3$–5, no C_6H_{14} derivative being obtained.[11] It would appear that the steric requirement to accommodate the alkyl chains within the hexagonal Mn_3Fe_3 cavities cannot be satisfied for $n > 5$. In the event this cavity is occupied by two CH_3 approaching from opposite sides and, at a greater distance, by four others.

Magnetic properties

The magnetic susceptibility of a polycrystalline sample fitted from 150 to 300 K (Fig. 4) conforms closely to the Curie–Weiss law, with the Curie constant $C = 70.13(4)$ J K T^{-2} mol^{-1} and Weiss constant $\theta = -100.26(3)$ K. The large negative value of θ clearly signals antiferromagnetic near-neighbour exchange. Below 100 K the inverse susceptibility increasingly deviates from Curie–Weiss behaviour, passing through a broad minimum at 55 K (Fig. 4). We have shown previously that such a maximum occurs at the same temperature for eight compounds of the type $AMnFe(C_2O_4)_3$ that have the honeycomb layer structure[11] so it is associated with the build-up of two-dimensional antiferromagnetic correlations. The value of the Curie constant calculated for two $S = \frac{5}{2}$ ions per formula unit, each with $g = 2$, is 87.5 J K T^{-2} mol^{-1}, distinctly larger than the measured value. Since it is unlikely that the g values deviate strongly from 2 for these d^5 ions, it appears that short-range antiferromagnetic correlations contribute to the measured susceptibility even above 150 K.

Below 27 K there is an abrupt increase in the polycrystalline

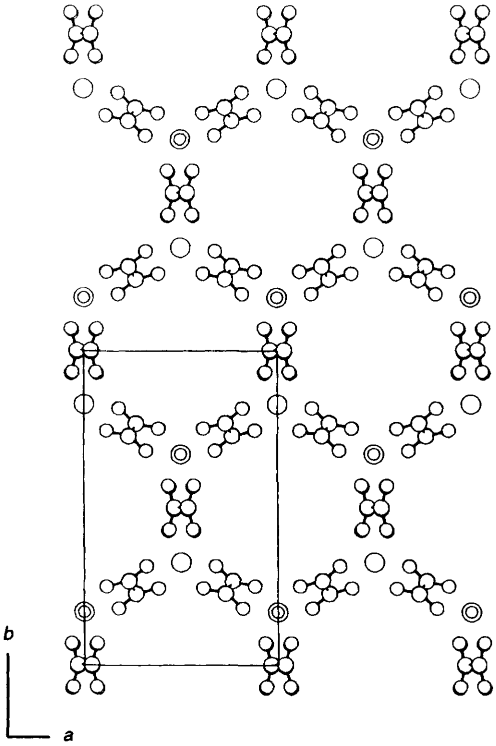

Fig. 1 Projection of the bimetallic tris(oxalate) layer in $N(n\text{-}C_5H_{11})_4MnFe(C_2O_4)_3$ along the c axis

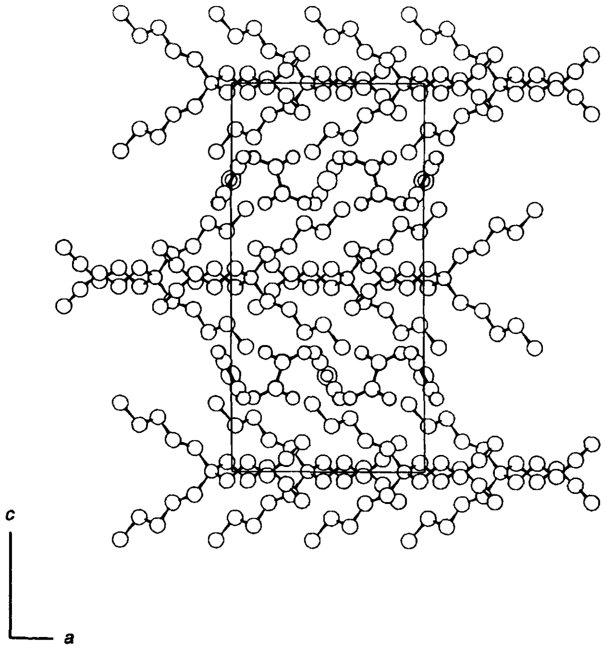

Fig. 2 Projection of the structure of $N(n\text{-}C_5H_{11})_4MnFe(C_2O_4)_3$ along the b axis

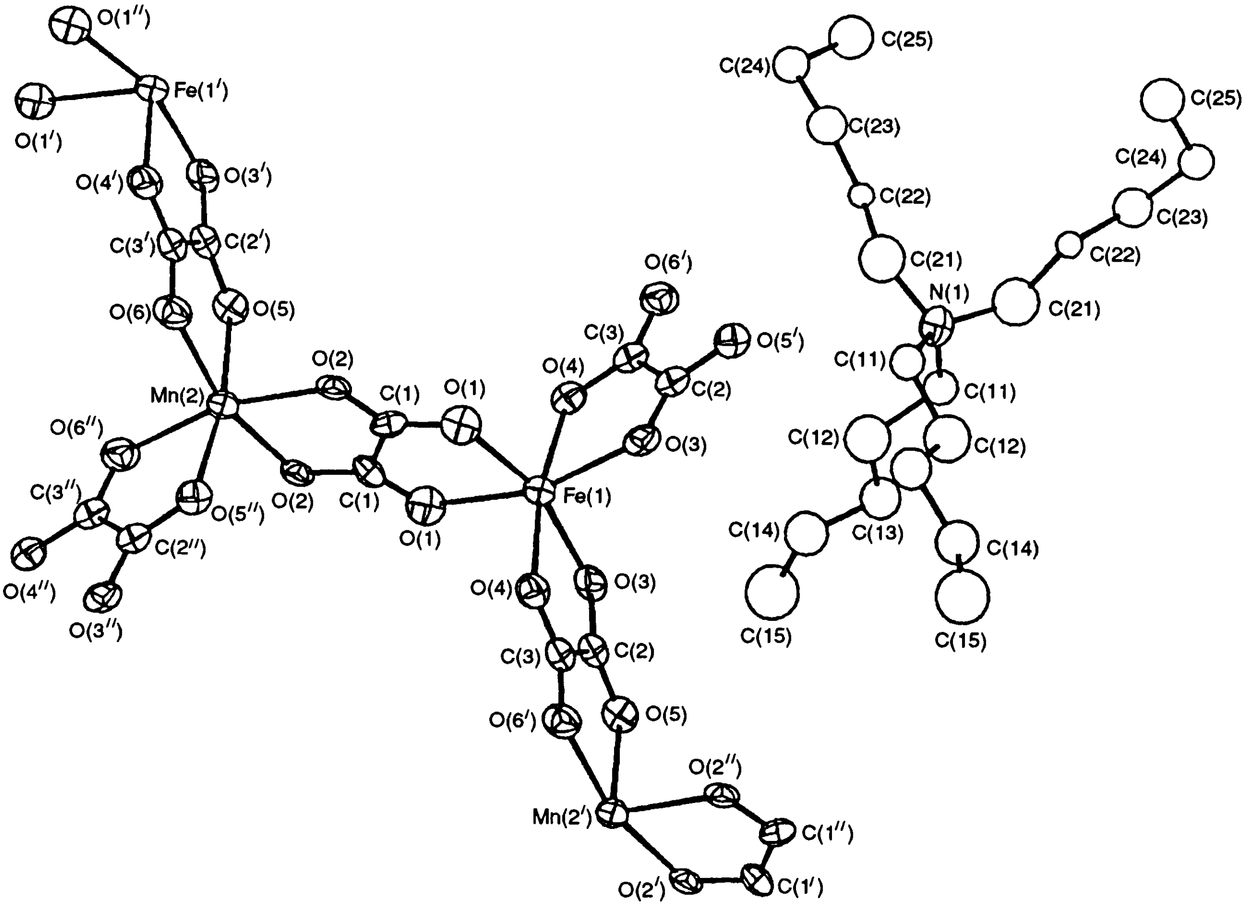

Fig. 3 The asymmetric unit in N(n-C_5H_{11})$_4$MnFe(C_2O_4)$_3$ with atom numbering

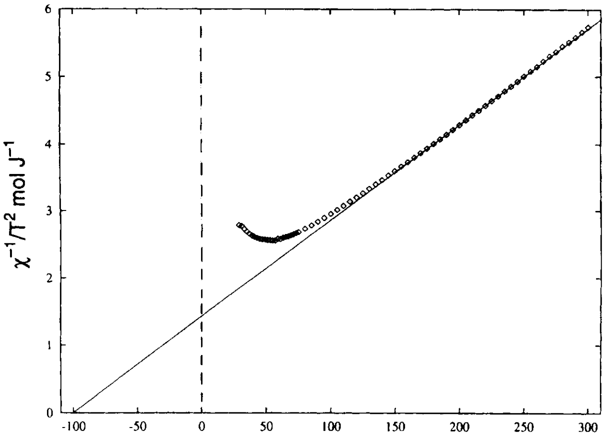

Fig. 4 Temperature dependence of the inverse susceptibility of polycrystalline N(n-C_5H_{11})$_4$MnFe(C_2O_4)$_3$ from 30 to 300 K. The straight line is the Curie–Weiss fit

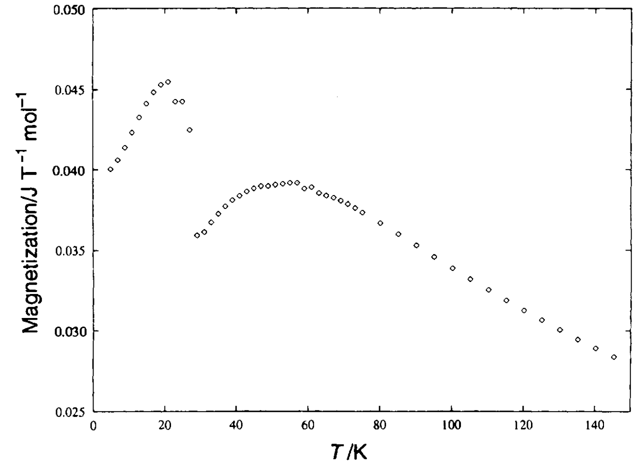

Fig. 5 Temperature dependent magnetization of polycrystalline N(n-C_5H_{11})$_4$MnFe(C_2O_4)$_3$ from 4 to 150 K

magnetization (Fig. 5), of the kind that we have observed previously in Mn($C_nH_{2n+1}PO_3$)·H_2O (n = 1–4),[10] and attributed to the onset of long-range antiferromagnetic order accompanied by spin canting. A requirement for the observation of a canted structure is that no centre of inversion exists between neighbouring sites of the magnetic ions. In the present case, not only are the modes of distortion around the two sites different but the metal ions are too. Thus the symmetry condition for canting is clearly satisfied in the present case. However, although they are both $3d^5$ ($^6A_1$) ions, small differences in their g values and single-ion anisotropy parameters are to be expected, so an alternative explanation for the low-temperature magnetic behaviour could be that the moments remain collinear, but differ slightly in magnitude.

Fig. 6 shows the magnetization of a single crystal of N(n-C_5H_{11})$_4$MnFe(C_2O_4)$_3$ recorded with the field (100 G) along three orthogonal axes. The axes were identified by Weissenberg photography of the crystal used. The temperature dependence of the moment is consistent with a second-order transition as expected for a transition to a long-range ordered state. It is clear that the major component of the uncompensated moment is parallel to the c axis, *i.e.* perpendicular to the [MnFe(C_2O_4)$_3$]$^-$ planes. Given the small uncertainties in crystal orientation, it is not clear whether the small values in the other two directions represent a true contribution to the canted moment. On the assumption that underlying magnetization parallel to c remains

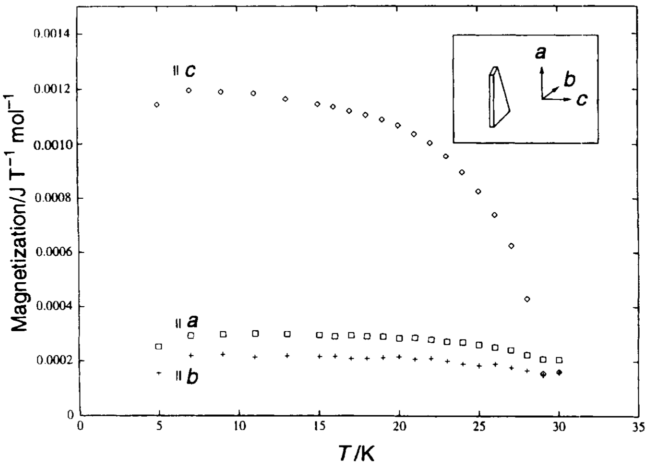

Fig. 6 Temperature-dependent magnetization of a single crystal of $N(n\text{-}C_5H_{11})_4MnFe(C_2O_4)_3$ from 5 to 30 K. Insert is the crystal used and the axis identification

constant below 30 K the additional magnetization at 5 K represents a measured net magnetic moment of 9.8×10^{-4} J T^{-1} mol^{-1}, equivalent to μ_{ferro} 8.78×10^{-5} μ_B atom^{-1}. If this small value is interpreted as a canting, the angle between the moments of Mn and Fe is calculated as $\sin^{-1}(\mu_{ferro}/gS)$. Again taking $S = \frac{5}{2}$ and $g = 2$ this corresponds to 0.001°. This small value represents a minimum since an isotherm measured for a polycrystalline sample at 5 K shows that the magnetization is not saturated even at 7 T.

Conclusion

The compound $N(n\text{-}C_5H_{11})_4MnFe(C_2O_4)_3$ is a ferrimagnet the bulk magnetic properties of which in the paramagnetic region closely mimic those of a two-dimensional antiferromagnet because of the coincidence of the ground states of the two metal ions. Its hexagonal network layer structure is similar to that found in bimetallic tris(oxalato)-complexes of Cr and Mn, though with a small orthorhombic distortion of the hexagonal symmetry. Below 27 K we find an uncompensated moment perpendicular to the layers equivalent to 8.78×10^{-5} μ_B atom^{-1} which could arise either from spin canting (estimated as 0.001°) or a small difference in the g values and single-ion anisotropy parameters of the two ions.

Acknowledgements

We acknowledge EPSRC and the EU Human Capital and Mobility Programme for support. We are grateful to Mr. C. J. Kepert for a Weissenberg photograph of the crystal used in the magnetic measurements.

References

1 M. Julve, J. Faus, M. Verdaguer and A. Gleizes, *J. Am. Chem. Soc.*, 1984, **106**, 8306.
2 See, for example, O. Kahn, *Molecular Magnetism*, VCH, New York, 1994.
3 H. Tanaki, Z. J. Zhong, N. Matsumoto, S. Kida, N. Koikawa, Y. Achiwa, Y. Hashimoto and H. Okawa, *J. Am. Chem. Soc.*, 1992, **114**, 6974.
4 S. Descurtins, H. W. Schmalle, H. R. Oswald, A. Linden, J. Ensling, P. Gütlich and A. Hauser, *Inorg. Chim. Acta*, 1994, **216**, 65.
5 See J. B. Goodenough, *Magnetism and the Chemical Bond*, Interscience, New York, 1963.
6 S. Descurtins, H. W. Schmalle, P. Schnewewly, J. Ensling and P. Gütlich, *J. Am. Chem. Soc.*, 1994, **116**, 9521.
7 L. O. Atovmyan, G. V. Shilov, R. N. Lyubovskaya, E. I. Zhilyaeva, N. S. Ovanesyan, S. I. Piramova and I. G. Gusakovskaya, *JETP Lett.*, 1993, **58**, 766.
8 See, for example, C. Bellitto and P. Day, *J. Mater. Chem.*, 1992, **2**, 265.
9 T. Moriya, *Phys. Rev.*, 1960, **117**, 635; **120**, 91.
10 S. G. Carling, P. Day and D. Visser, *J. Solid State Chem.*, 1993, **106**, 111.
11 C. Mathonière, C. J. Nuttall, S. G. Carling and P. Day, *Inorg. Chem.*, in the press.
12 J. C. Bailar and E. M. Jones, *Inorg. Synth.*, 1939, **1**, 37.
13 G. M. Sheldrick, SHELXL 93, Program for refining crystal data, University of Göttingen, 1993.

Received 5th *October* 1995; *Paper* 5/06572K